EoS studies in nucleus-nucleus collisions: from Coulomb barrier to LHC

M. Veselsky, J. Klimo (Institute of Physics, Slovak Academy of Sciences)

G.A. Souliotis (University of Athens)

X.G. Deng, Y.G. Ma (SINAP CAS Shanghai)

M. Ploskon (LBL Berkeley)

Nuclear Equation of State

Definition : *A relation that determines how nuclear matter (composing of neutrons & protons) behaves when subjected to different pressure, density & temperature*

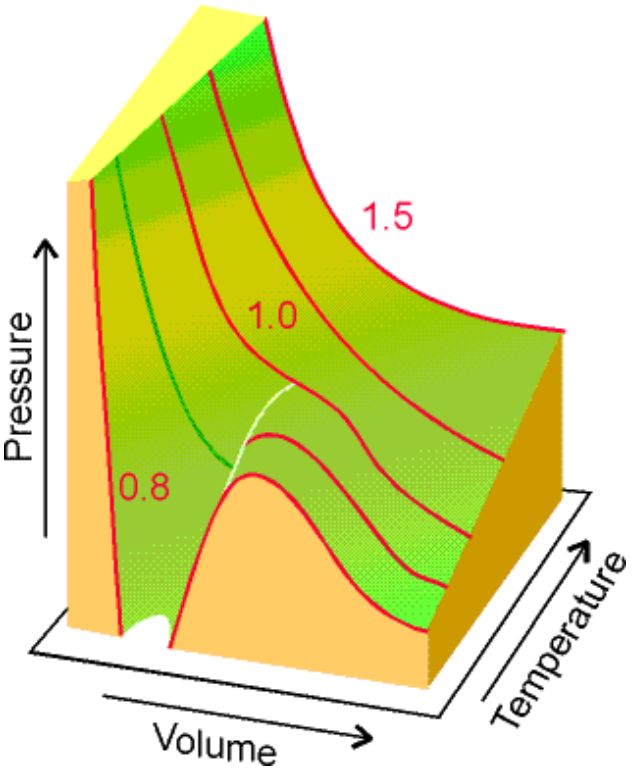

In real gas, this relation is very well known, because Van der Waals force the gas molecules is known. In nuclear matter interaction between nucleons is not very well known

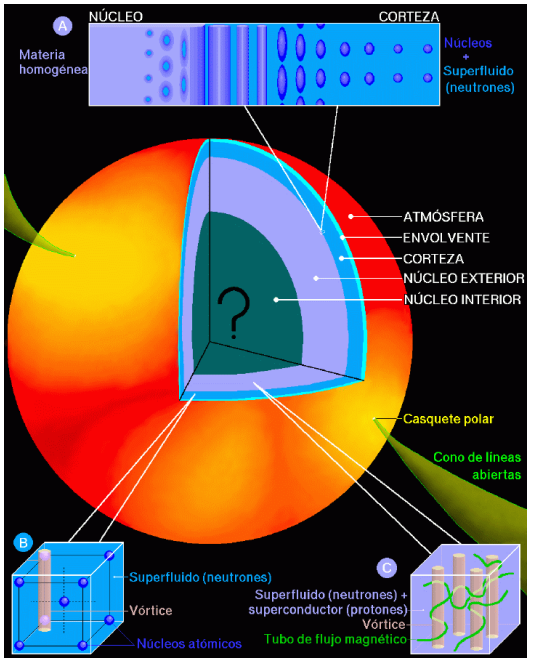

Nuclear equation of state is needed to understand properties of astrophysical objects (neutron stars, supernova) and to determine production site of heavy nuclei

Nucleus-nucleus collisions as a tool for EoS study

Nucleus-nucleus collisions at wide range of beam energies allow to study properties of nuclear matter by variation of density, temperature and isospin asymmetry of nuclear matter in participant regions.

Nuclear matter is a two-component system. Incompressibility at saturation density is the most important parameter of equation of state of symmetric nuclear matter. The effect of changing neutron-to-proton ratio is typically treated in terms of symmetry energy and its density dependence.

Various implementations of Boltzmann equation (Fokker-Planck equation, Boltzmann-Uehling-Uhlenbeck equation, Quantum Molecular Dynamics) are used for modeling of the nucleus-nucleus collisions and testing of various equations of state.

Successful equations of state can be used for modeling of astrophysical objects (neutron stars) and processes (supernova explosions)

Boltzmann-Uehling-Uhlenbeck equation

The BUU equation reads

EoS

$$\frac{\partial f}{\partial t} + v \cdot \nabla_r f - \nabla_r U \cdot \nabla_p f = \frac{4}{(2\pi)^3} \int d^3p_2 d^3p_3 d\Omega$$
$$\frac{d\sigma_{NN}}{d\Omega} v_{12} \times [f_3 f_4 (1-f)(1-f_2) - f f_2 (1-f_3)(1-f_4)]$$
$$\delta^3(p + p_2 - p_3 - p_4), \qquad (1)$$

where $f = f(r, p, t)$ is the phase-space distribution function. It is solved with the test particle method of Wong [15], with the collision term as introduced by Cugnon, Mizutani and Vandermeulen [16]. In Eq.(1), $\frac{d\sigma_{NN}}{d\Omega}$ and v_{12} are in-medium nucleon-nucleon cross section and relative velocity for the colliding nucleons, respectively, and U is the single-particle mean field potential with the addition of the isospin-dependent symmetry energy

Production Cross-Sections of SHE

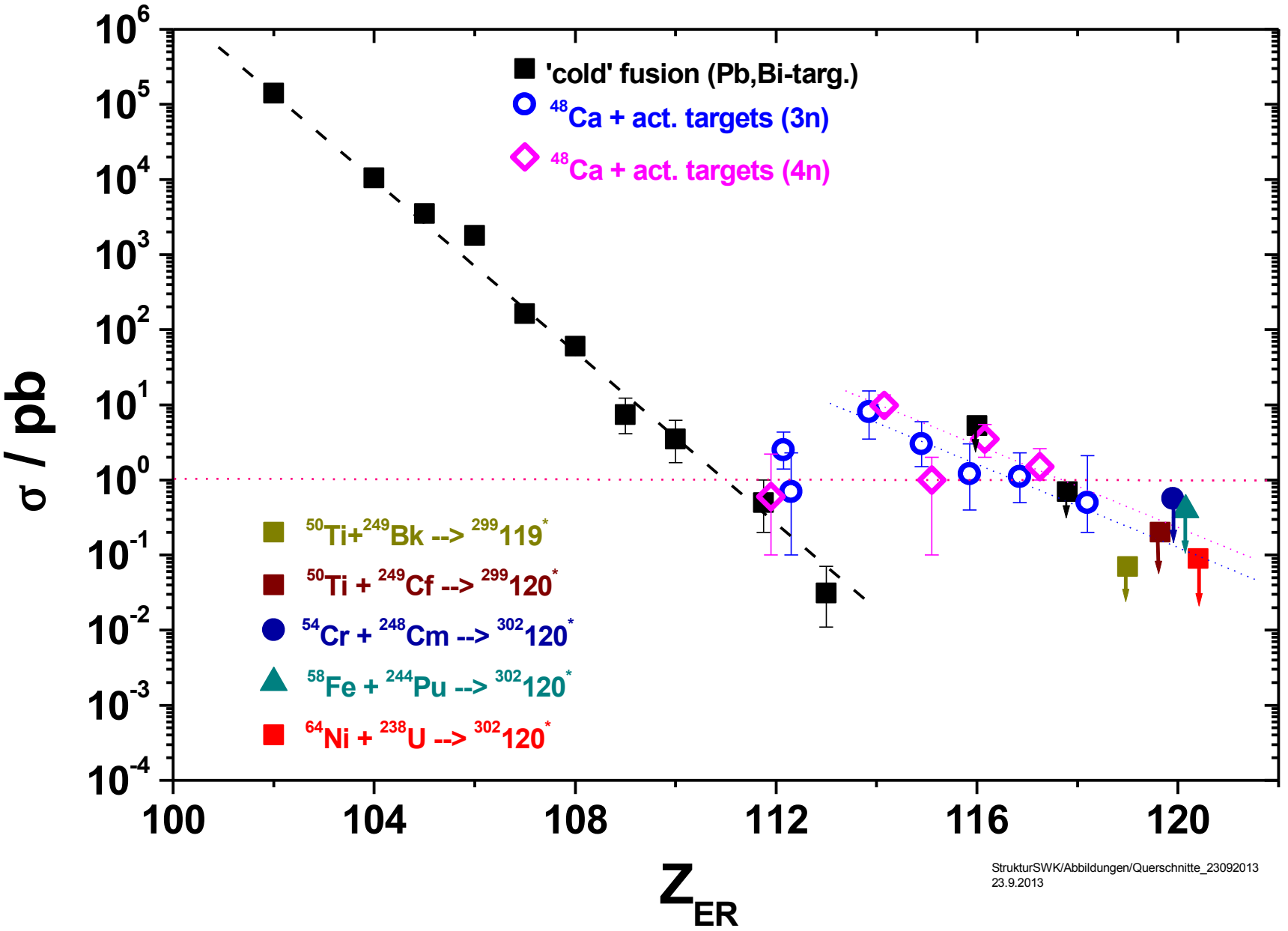

Production of superheavy nuclei

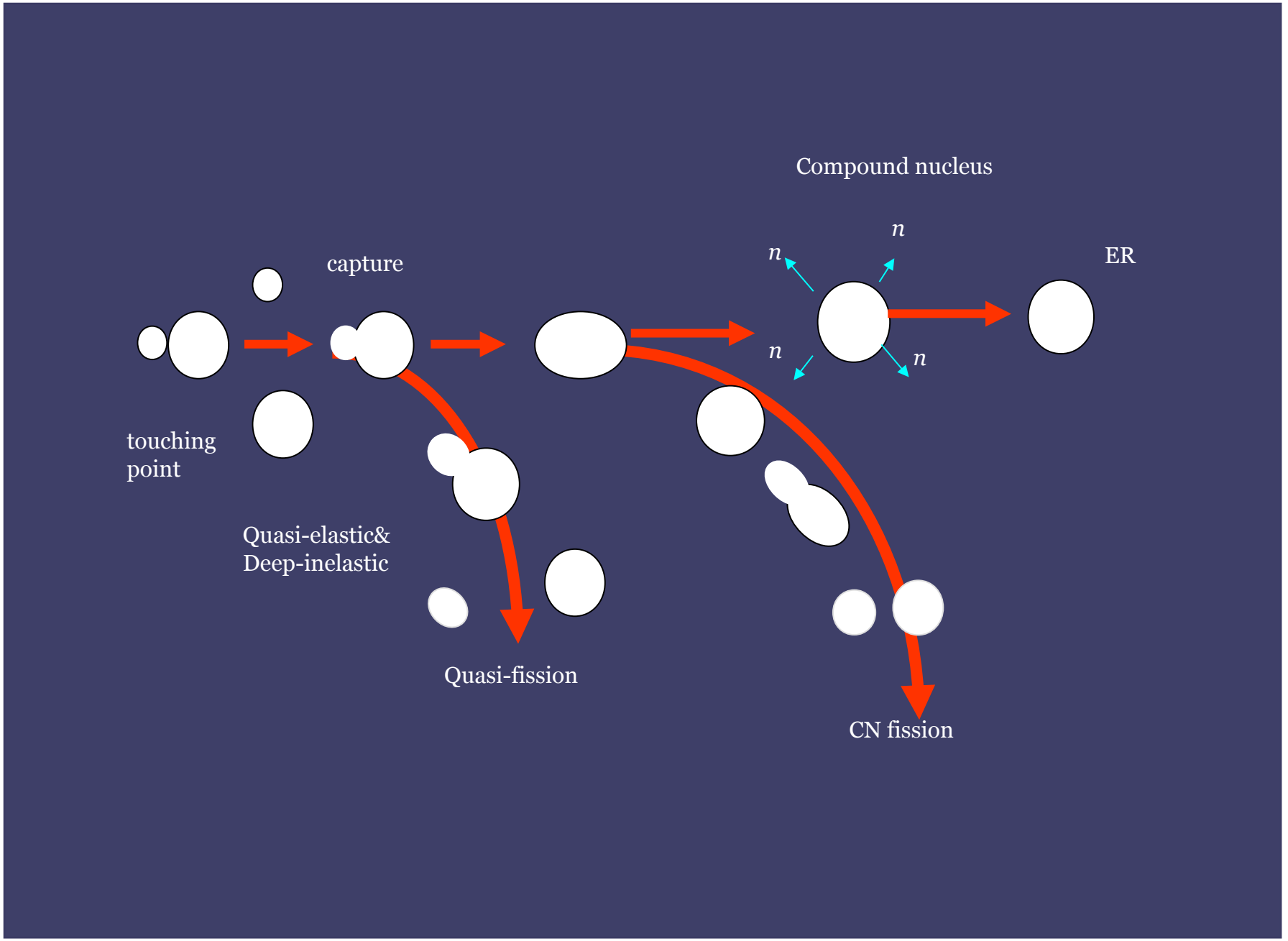

Competition between fusion and QF processes: Hs (Z=108) composite systems

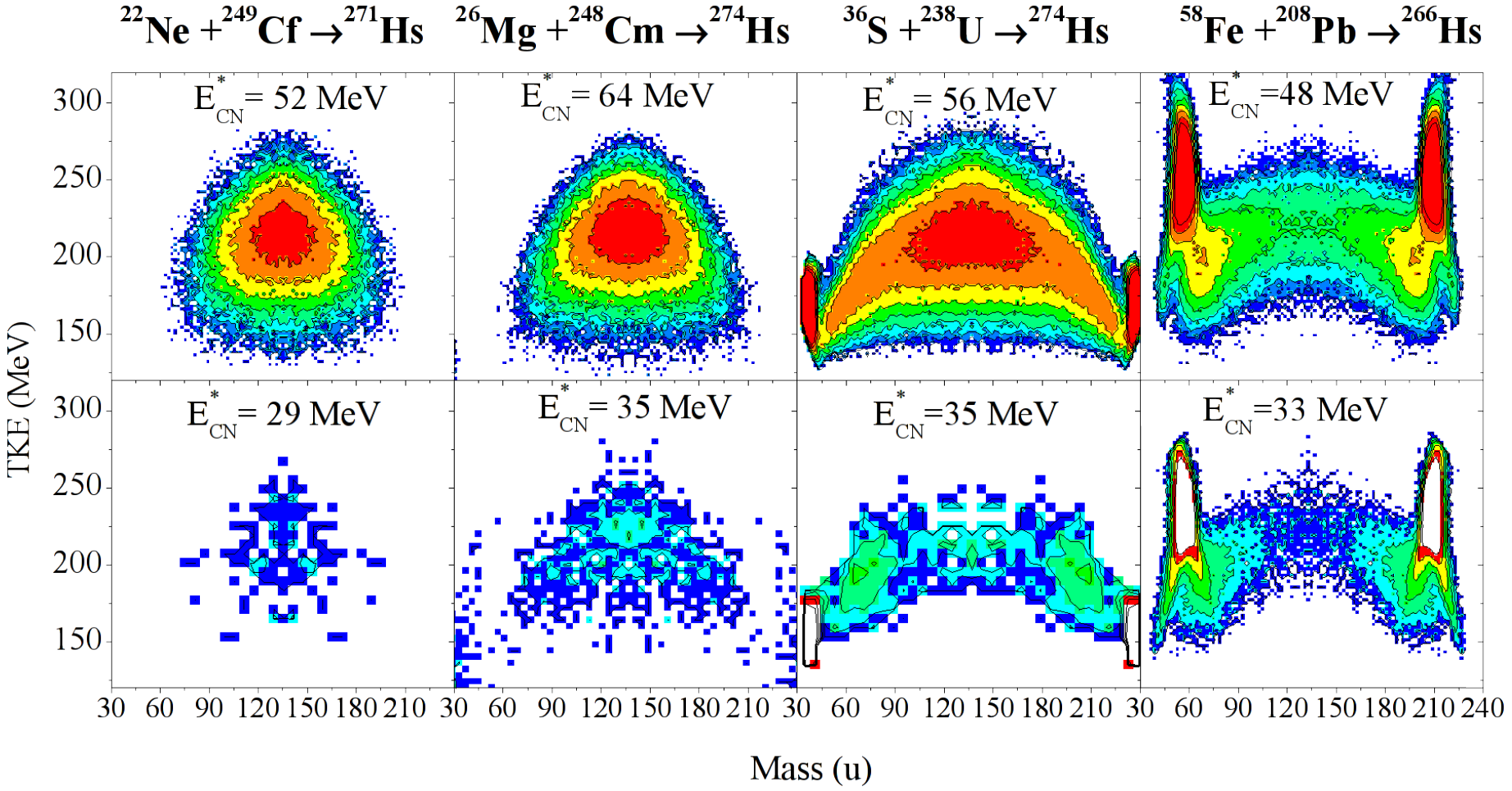

Z_1Z_2=980 1152 1472 2132

Experimental data from Itkis et al. (JINR Dubna)

BUU for low energy collisions :

EoS: $$U = a\rho + b\rho^{\kappa} + 2a_s(\frac{\rho}{\rho_0})^{\gamma}\tau_z I,$$

Pauli principle applied separately to protons and neutrons

Coulomb interaction taken into account, force acting in the cell obtained as a sum of contributions of particles outside of that cell, eventual interaction of particles within the cell considered in the collision term

In-medium cross sections either from EoS (M. Veselsky and Y.G. Ma, PRC 87 (2013) 034615) or free, practically no influence since collisions mostly Pauli blocked

Validated against CoMD

EoS vs incompressibility

Starting from potential

$$U = a(\frac{\rho}{\rho_0}) + b(\frac{\rho}{\rho_0})^{\kappa}$$

After applying standard conditions for saturation we arrive to solution

$$a = \frac{2(-\kappa B - \frac{3}{5}(\kappa - \frac{2}{3})\epsilon_F(\rho_0))}{\kappa - 1}$$

$$b = \frac{\kappa + 1}{\kappa - 1}(B + (\frac{1}{5})\epsilon_F(\rho_0))$$

And get incompressibility (linear to κ !)

$$K_0 = 9\kappa(B + \frac{\epsilon_F(\rho_0)}{5}) - \frac{6}{5}\epsilon_F(\rho_0)$$

Reactions ^{64}Ni+^{186}W,^{208}Pb,^{238}U, ^{48}Ca+^{208}Pb,^{238}U,^{249}Cf at 5 AMeV

Incompressibilities between 200 – 360 MeV considered

Symmetry energy density dependences between γ = 0.5 – 1.5 considered

Simulations at 5 AMeV for b = 0.5 fm

Time evolution running until 3000 fm/c

600 test particles for each run, 20 runs per case

Computational workstation using 4 Xeon Phi coprocessor cards used (61 cores per card)

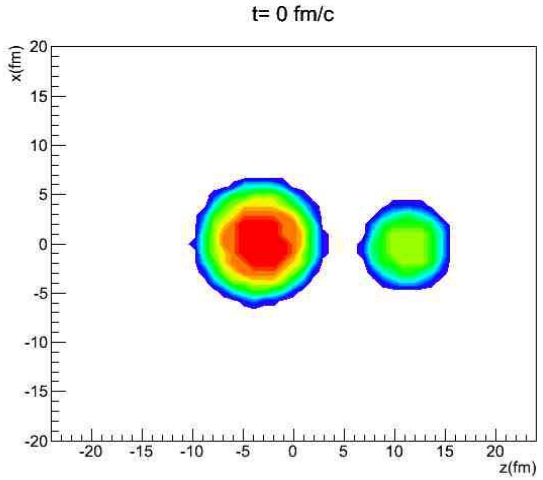

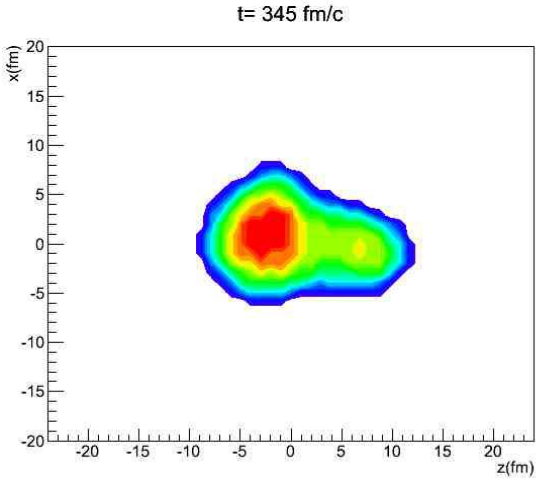

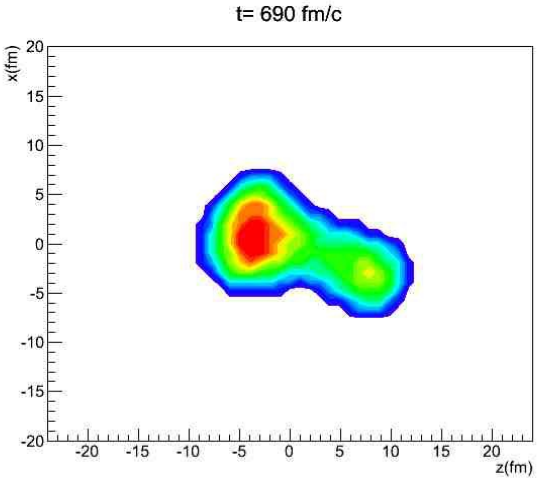

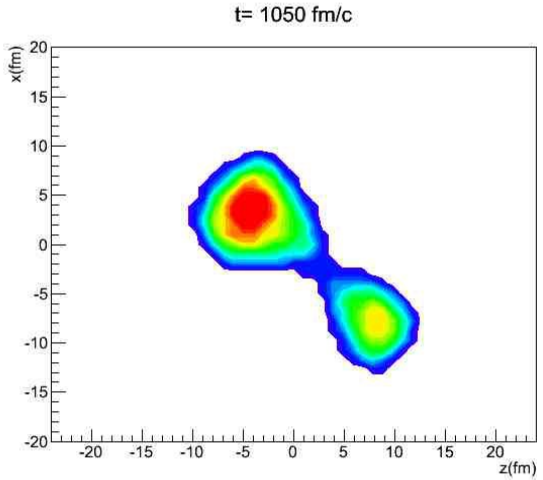

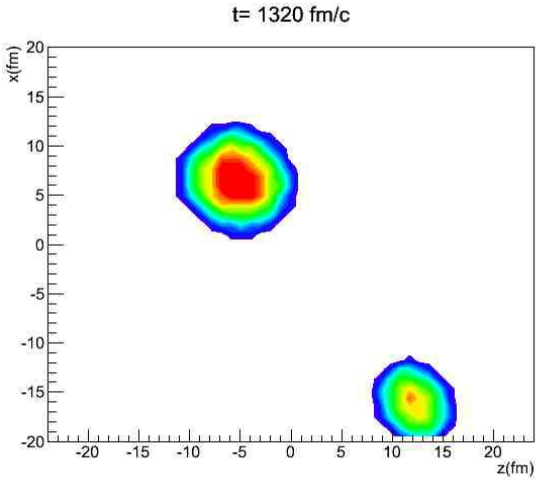

$K_0 = 200$ MeV, γ=0.5

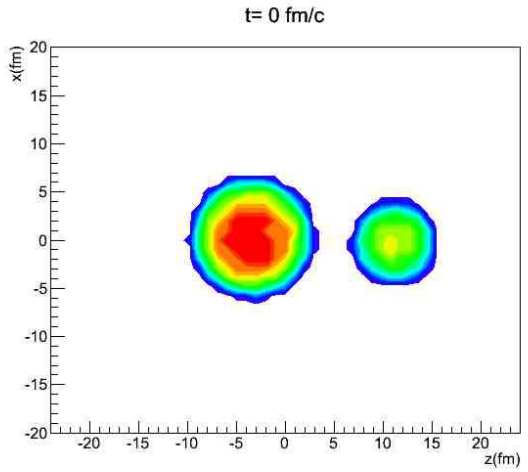

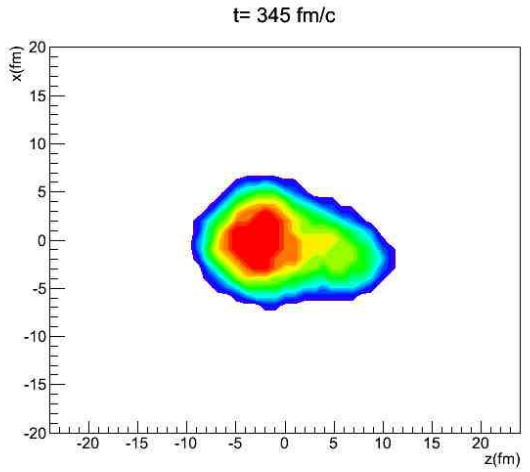

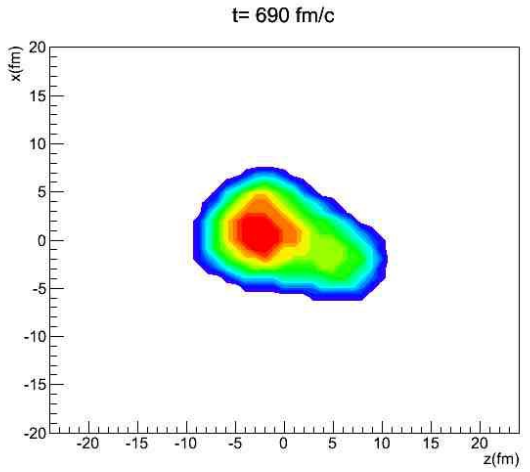

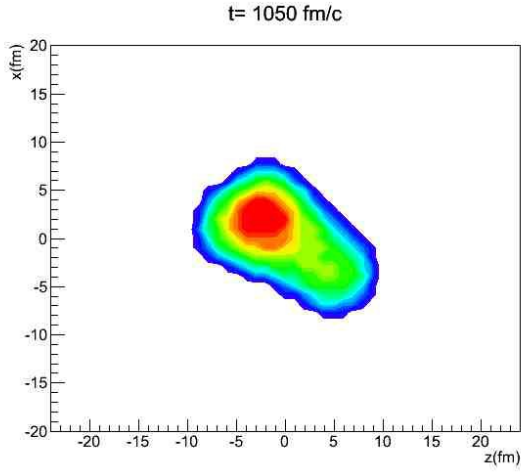

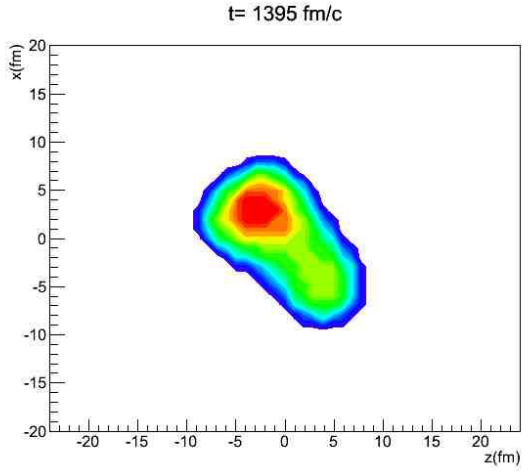

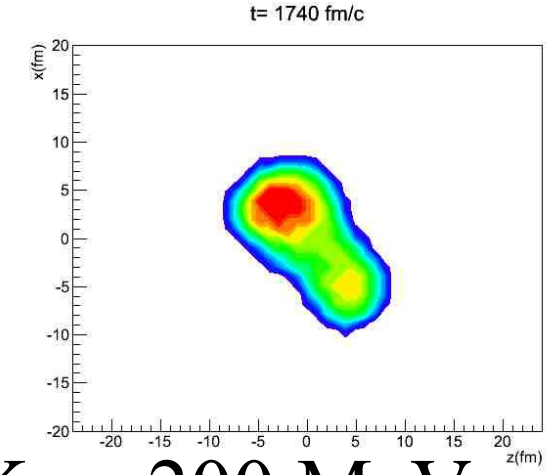

$K_0 = 200$ MeV, γ=1.5

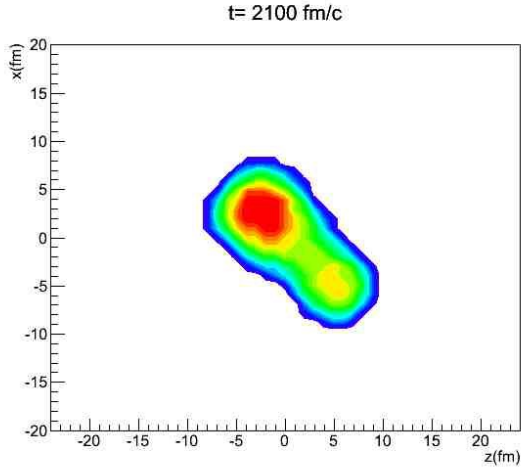

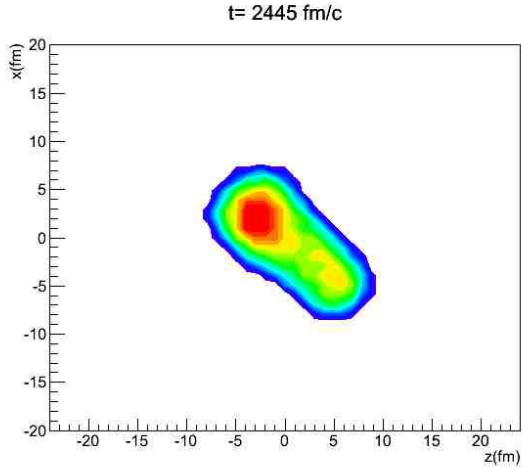

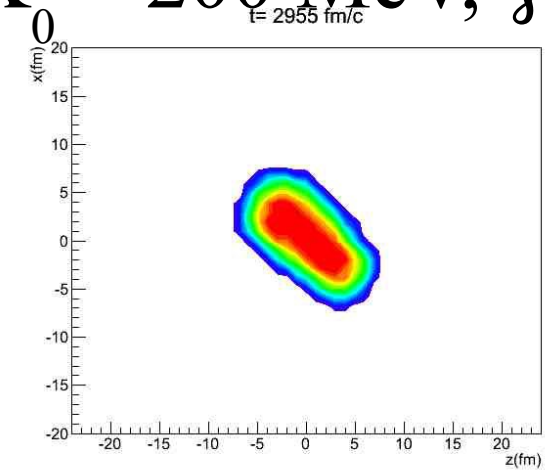

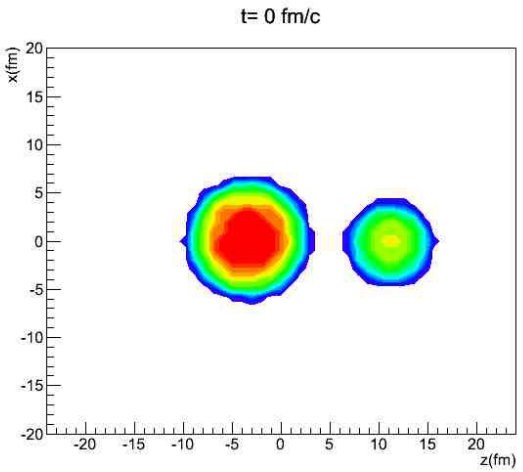

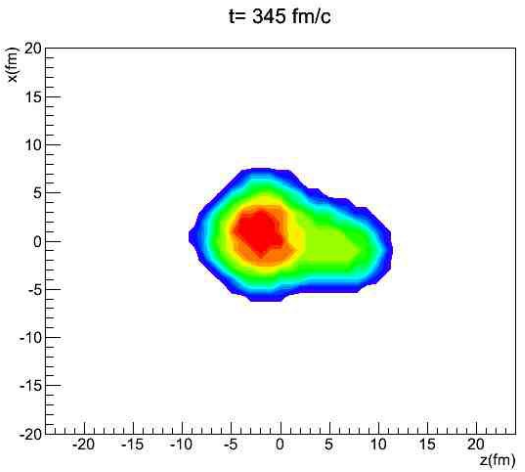

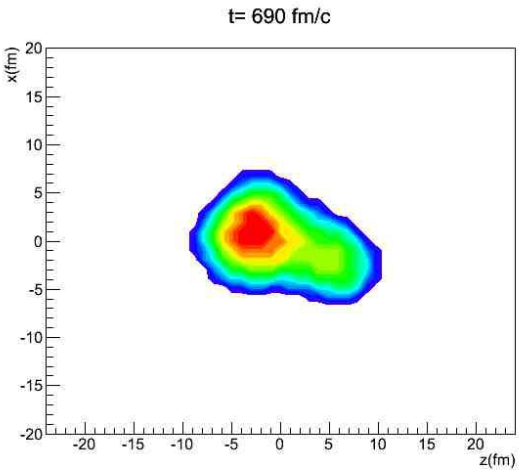

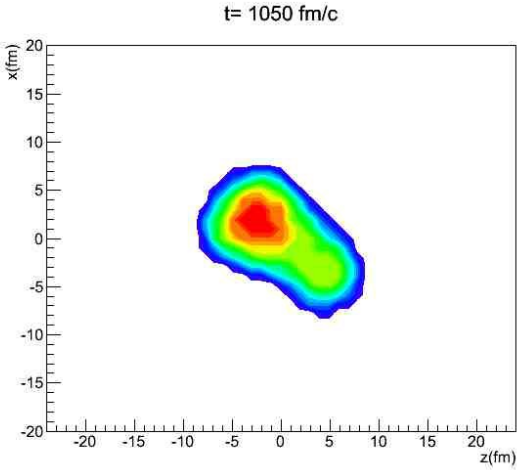

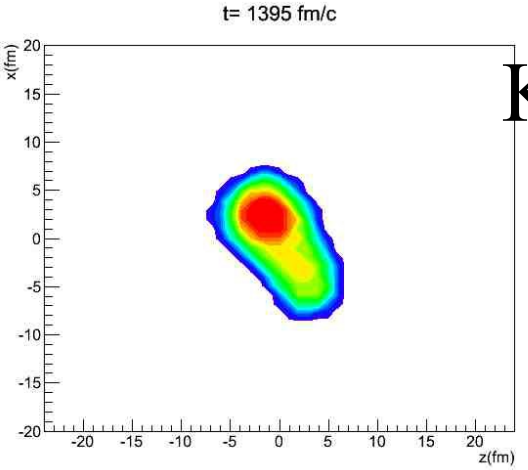

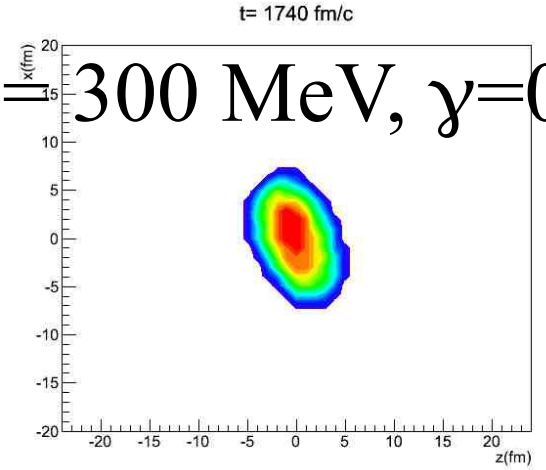

K_0 = 300 MeV, γ=0.5

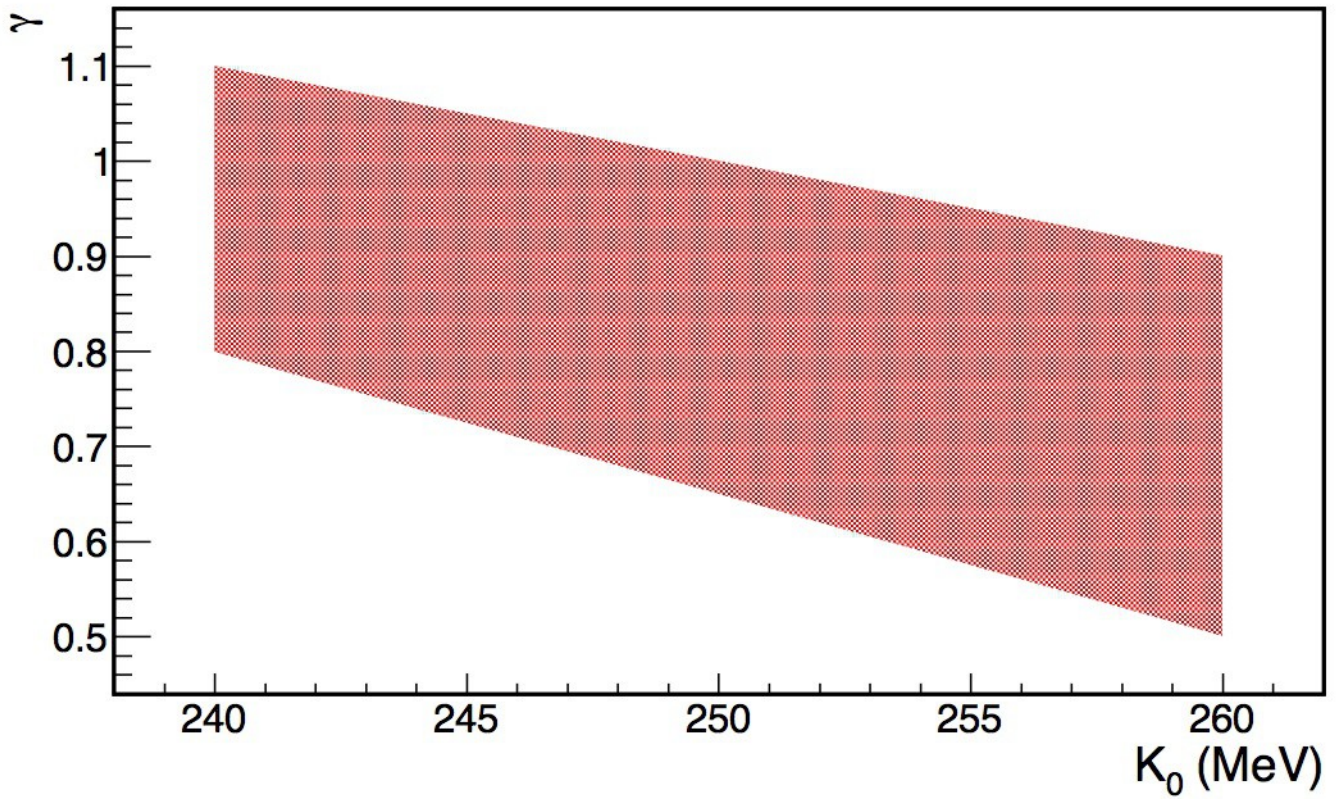

Summary constraints on incompressibility and density dependence of symmetry energy

Narrow range of incompressibility between 240-260 MeV (for density range 0 – 1.4 ρ_0)

Stiff density dependences of symmetry energy with $\gamma > 1$ rejected, constrained range anti-correlates with incompressibility

In-medium cross section from EoS:

Method:

Formally transform EoS into Van der Waals form, then perform inversion and extract the proper (excluded) volume for each density, temperature and isospin.

M. Veselsky and Y.G. Ma, PRC 87 (2013) 034615

$$p = \rho T + a\rho^2 + b\kappa\rho^{1+\kappa} + 2\gamma a_s \rho_0 (\frac{\rho}{\rho_0})^{1+\gamma}\tau_z I$$

When looking for relation of equation of state and emission rates one can consider the van der Waals equation of state. It is written as

$$(p + a'\rho^2)(V - Nb') = NT \tag{4}$$

or

$$(p + a'\rho^2)(1 - \rho b') = \rho T \tag{5}$$

where the parameter a' is related to attractive interaction among particles and b' represents the proper volume of the constituent particles. In geometrical picture the volume of the particle can be directly related to its cross section for interaction with particles. It is possible to formally transform the equation of state of asymmetric nuclear matter (and practically any equation of state of any form) into the van der Waals equation. Then one obtains coefficients

$$a' = -a \tag{6}$$

and

$$b' = \frac{b\kappa\rho^\kappa + 2\gamma a_s(\frac{\rho}{\rho_0})^\gamma \tau_z I}{p - a\rho^2} = \frac{b\kappa\rho^\kappa + 2\gamma a_s(\frac{\rho}{\rho_0})^\gamma \tau_z I}{\rho T + b\kappa\rho^{1+\kappa} + 2\gamma\rho_0 a_s(\frac{\rho}{\rho_0})^{1+\gamma}\tau_z I} \tag{7}$$

where the latter provides a measure of the proper volume of the constituent of the gas, nucleon in this case, as a measure of deviation from its behavior of the ideal gas. The proper volume of nucleon can be used to estimate its cross section within the nucleonic medium

$$\sigma = 1.209\ b'^{2/3} \tag{8}$$

which can be implemented into the collision term of the BUU equation.

Semi-stiff EoS (K_0=270 MeV)

Semi-stiff Esym (γ=1.)

Directed flow:

symbols- calc.

line - experiment

Elliptic flow:

Symbols - calc.

line - experiment

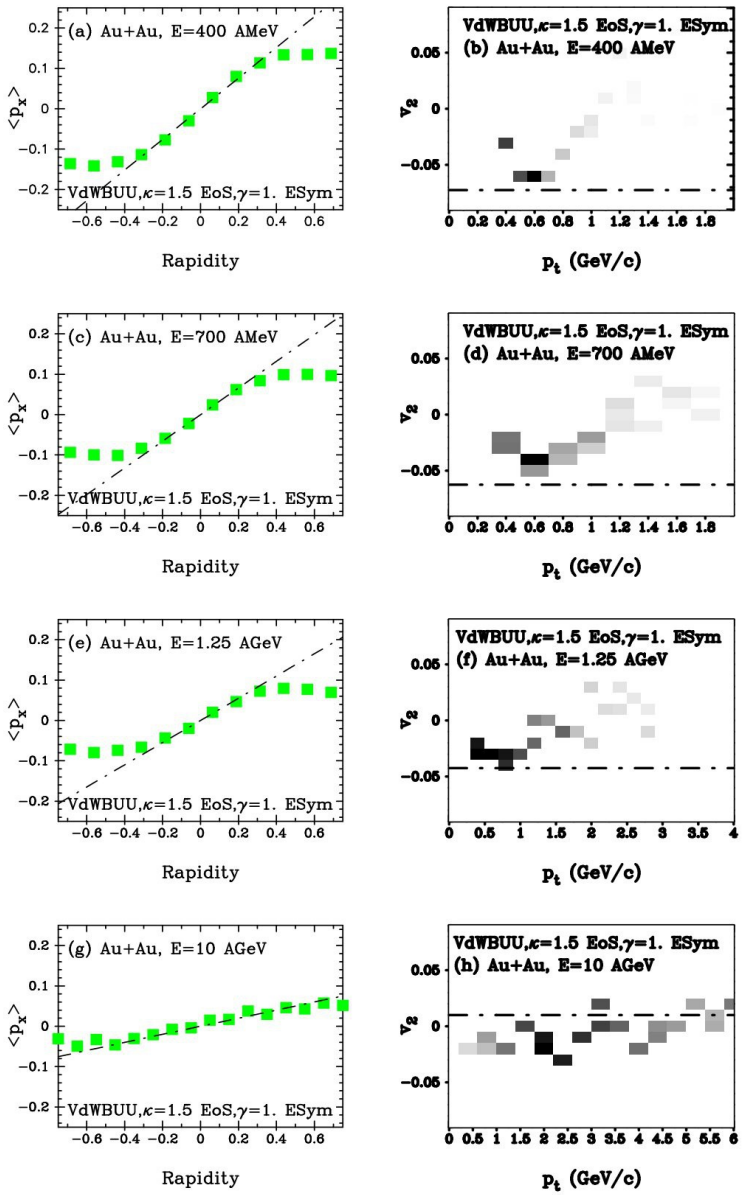

FIG. 4: Systematics of the proton directed flow (left panels, lines indicate experimentally observed slopes) and the momentum dependence of the calculated proton elliptic flow at mid-rapidity versus the experimental value (boxes and the dash-dotted line in right panels, respectively) in the collisions of Au+Au at beam energies ranging from 400 AMeV to 10 AGeV. Results were obtained using the VdWBUU simulation using the intermediate EoS with $\boldsymbol{\kappa = 3/2}$ ($\boldsymbol{K_0}$=272 MeV) and the symmetry energy density dependence with $\boldsymbol{\gamma = 1}$.

EoS-dependent collision term (with in-medium cross sections) leads to correct (positive) directed flow, while free cross sections lead to incorrect (negative) directed flow !!!

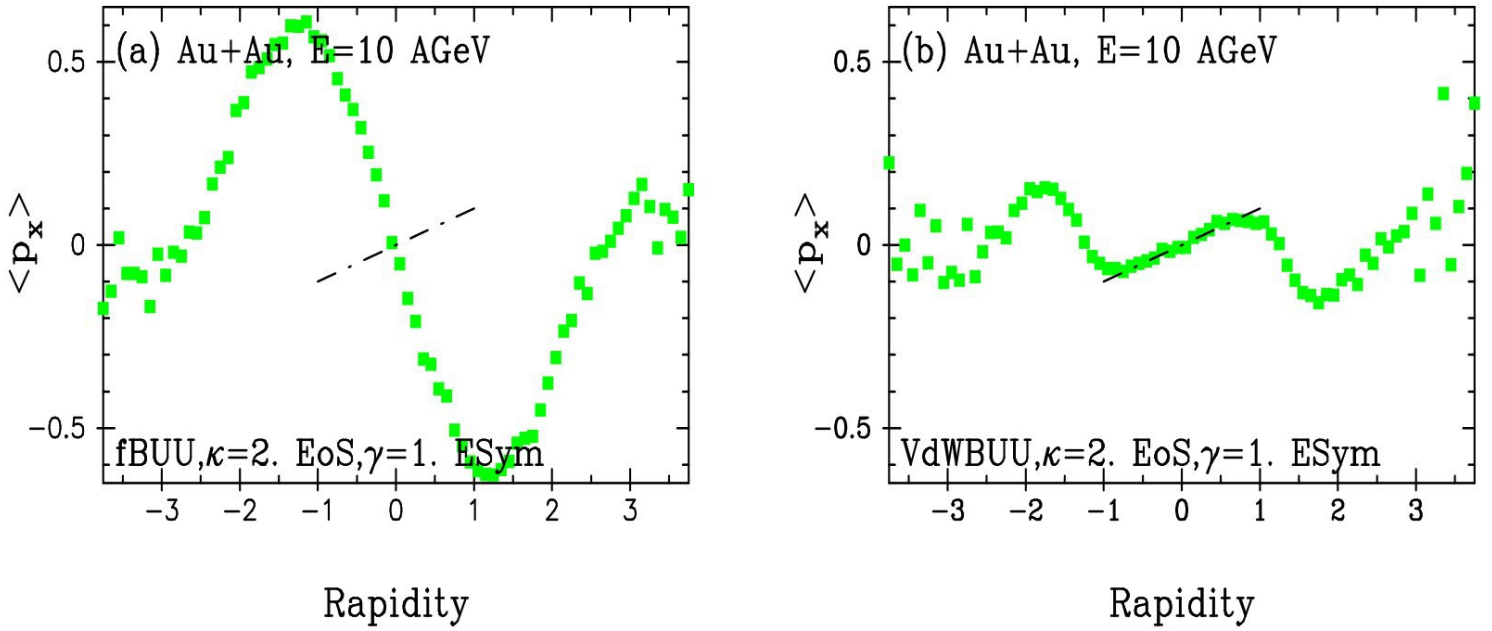

FIG. 2: Proton directed flow in the collisions of Au+Au at beam energy of 10 AGeV. Results were obtained using the simulation with and without EoS-dependent in-medium nucleon-nucleon cross sections (left and right panels, respectively) using the stiff EoS with $\kappa = 2$ (K_0=380 MeV) and the symmetry energy density dependence with $\gamma = 1$. Lines indicate experimentally observed slope.

When combined with similar analysis using the flow observables between 0.4 – 10 AGeV

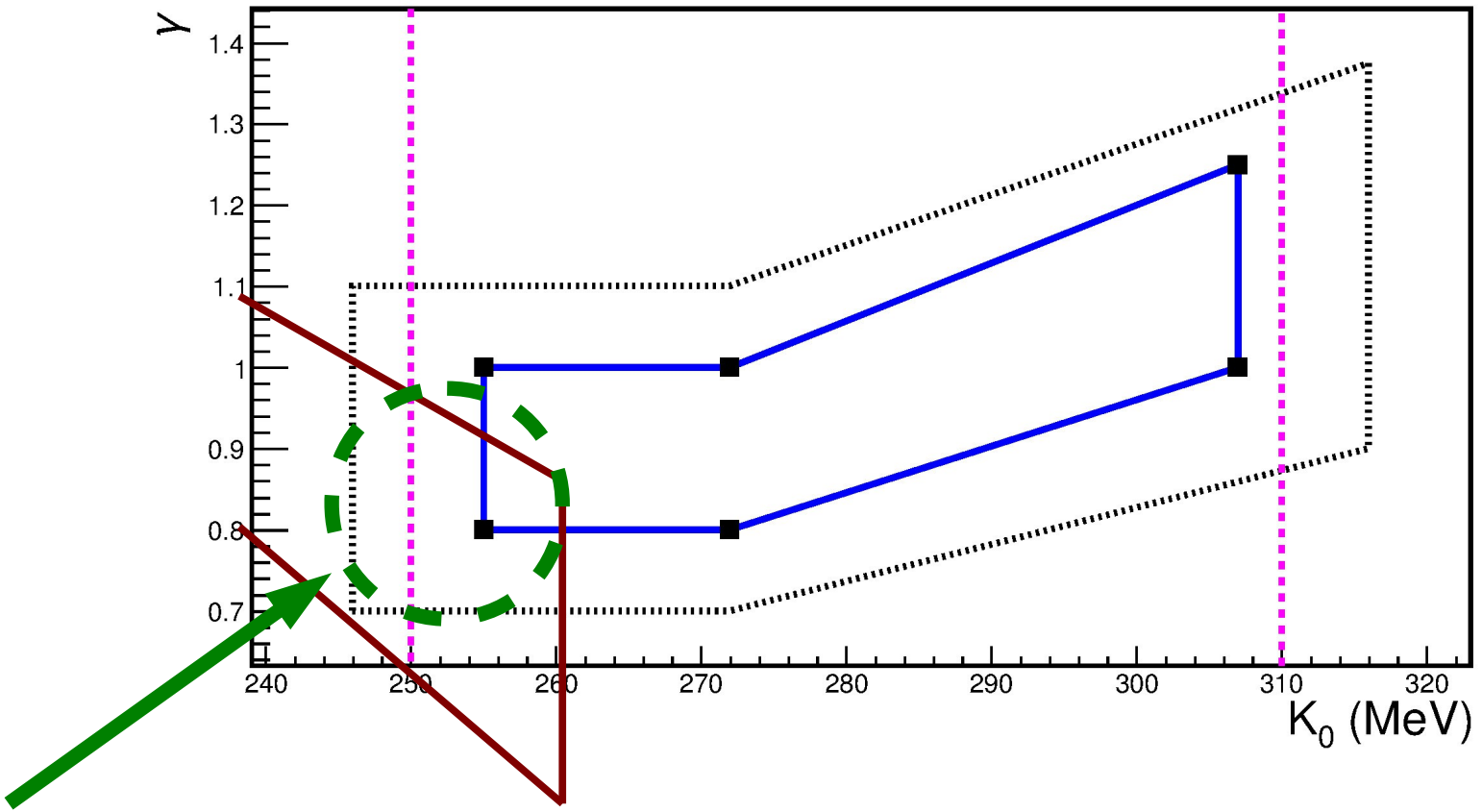

Combined constraint for 0 – 5 ρ_0

Transport coefficients from EoS

(X.G. Deng, Y.G. Ma, M.V., PRC 94, 044622 (2016))

Shear viscosity (momentum transport)

Isospin diffusivity (particle transport)

Heat conductivity (heat transport)

Central collisions of Au+Au at 100 – 300 AMeV

Formulas from Bertsch, Das Gupta, Phys. Rep. 160, 189 (1988).

Scaled by in-medium vs free nucleon-nucleon cross section.

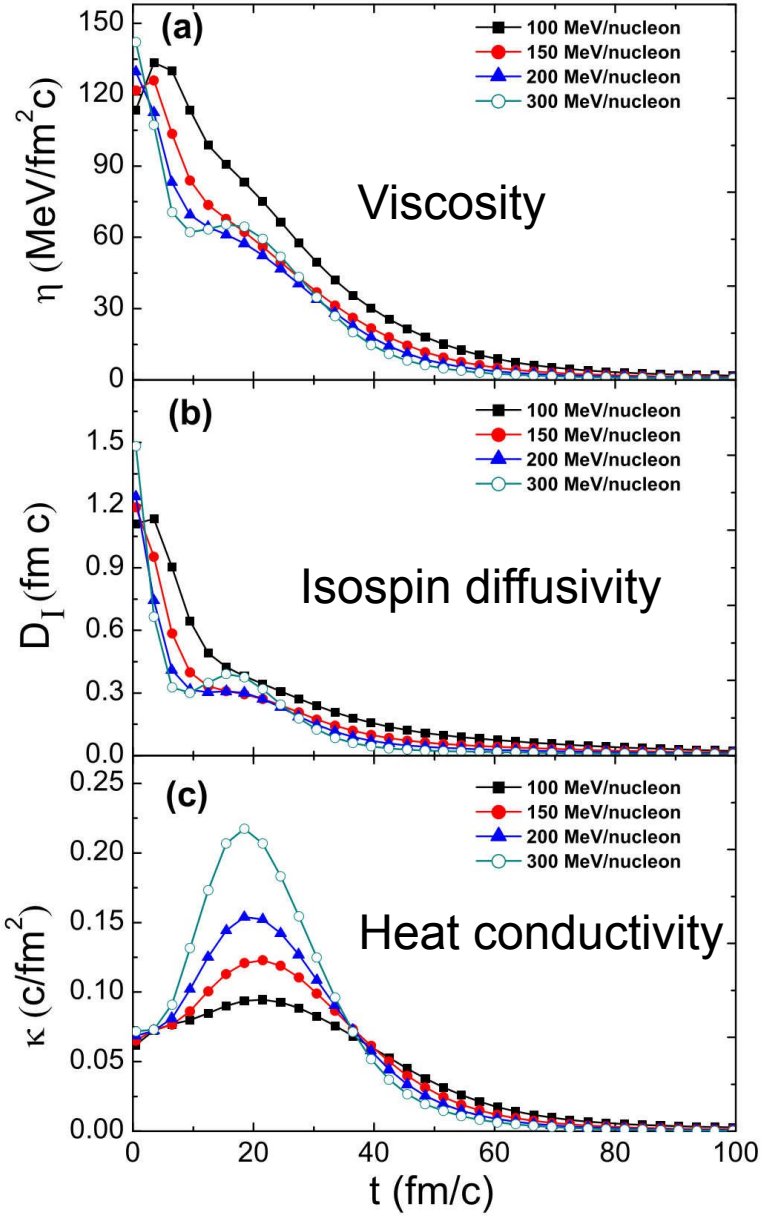

FIG. 4. Time evolution of the shear viscosity (a), isospin diffusivity (b), and heat conductivity (c) at different incident energies for the soft EoS in the region of $X[-5,5]$, $Y[-5,5]$, and $Z[-5,5]$.

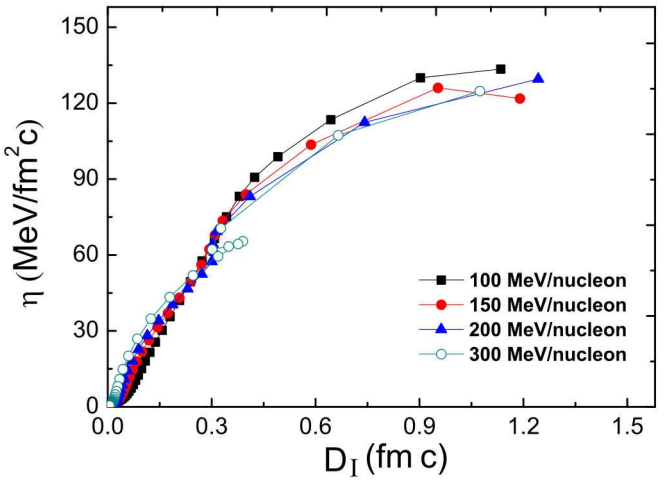

FIG. 9. Shear viscosity as a function of isospin diffusivity at different incident energies for the soft EoS in the region of $X[-5,5]$, $Y[-5,5]$, $Z[-5,5]$.

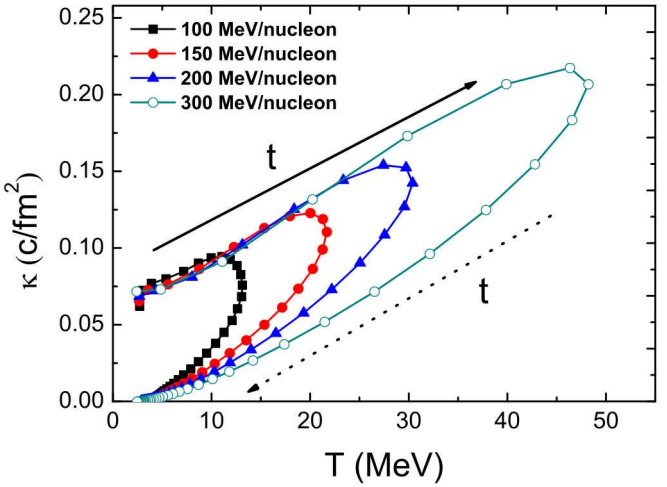

FIG. 10. Heat conductivity as a function of temperature at different incident energies for the soft EoS in the region of $X[-5,5]$, $Y[-5,5]$, and $Z[-5,5]$. Filled and dotted arrows indicate the compression process and expansion process, respectively.

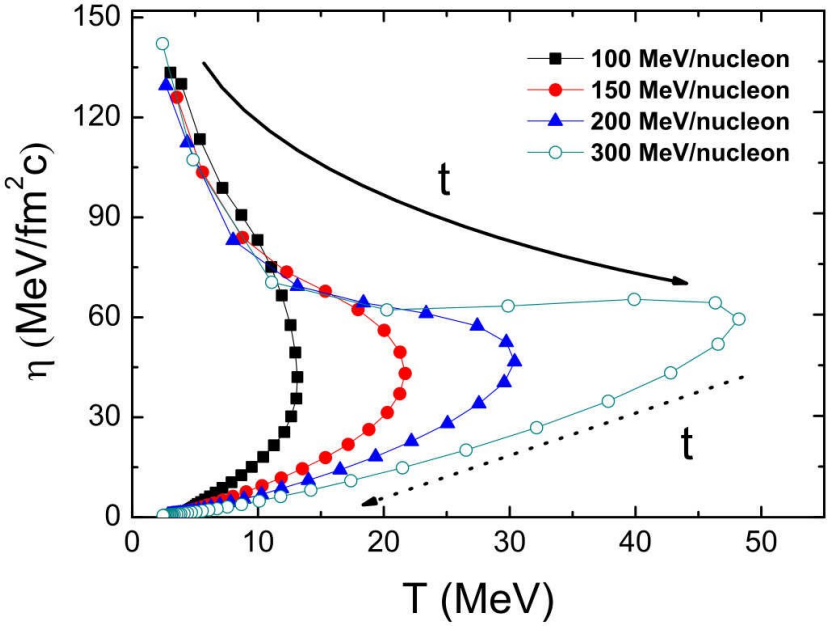

FIG. 11. Shear viscosity as a function of temperature at different incident energies for the soft EoS in the region of $X[-5,5]$, $Y[-5,5]$, and $Z[-5,5]$. Filled and dotted arrows indicate the compression process and expansion process, respectively.

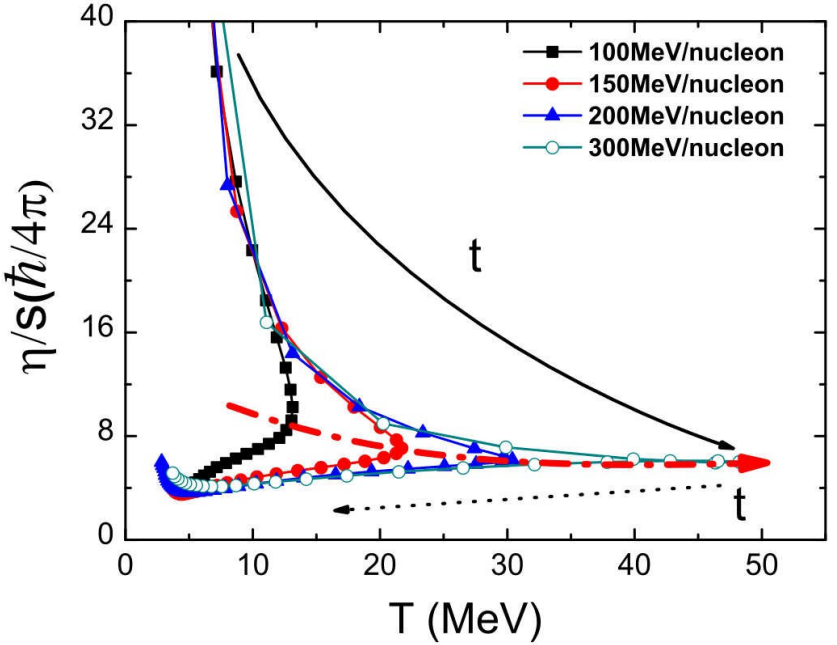

FIG. 12. Ratio of the shear viscosity to the entropy density, in units of $\frac{\hbar}{4\pi}$, as a function of the temperature at different incident energies for the soft EoS in the region of $X[-5,5]$, $Y[-5,5]$, and $Z[-5,5]$. The dashed red line shows the trend of the η/s value at the turning point with the temperature.

Liquid-like and gas-like branch (viscosity drops or grows with temperature)

Minimum of viscosity/entropy ratio at 6 times KSS bound

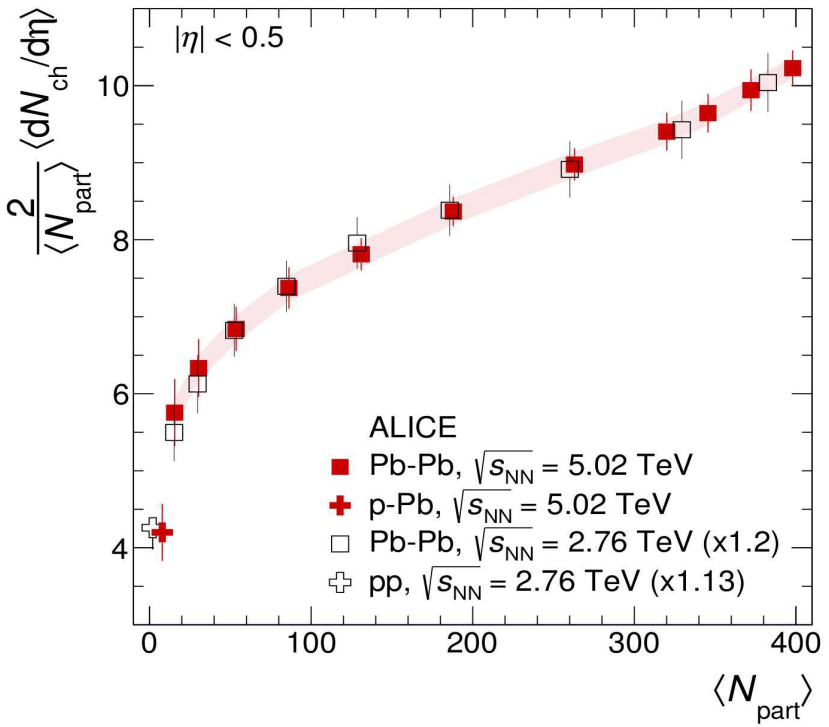

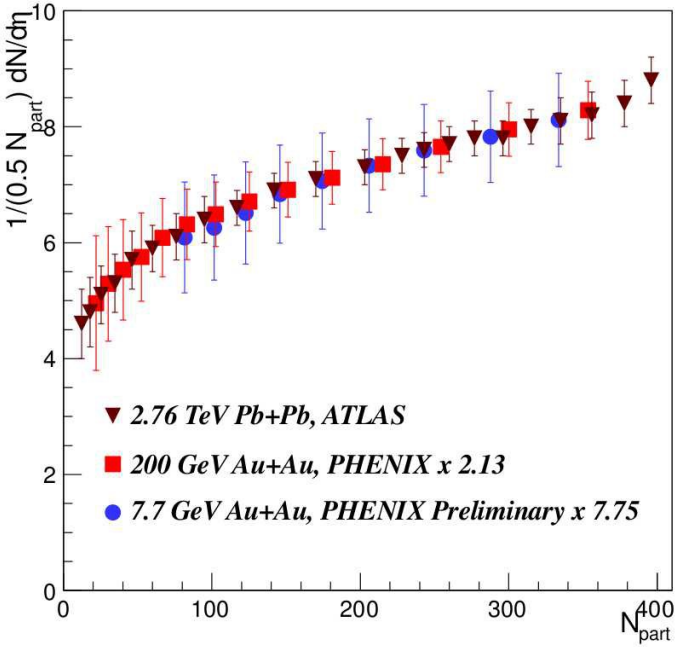

Ultrarelativistic nucleus-nucleus collisions

Shape of multiplicity distribution as a function of number of participating nucleons does not change within 3 orders of magnitude in beam energy !

Number of nucleon-nucleon collisions stays the same. Glauber picture.

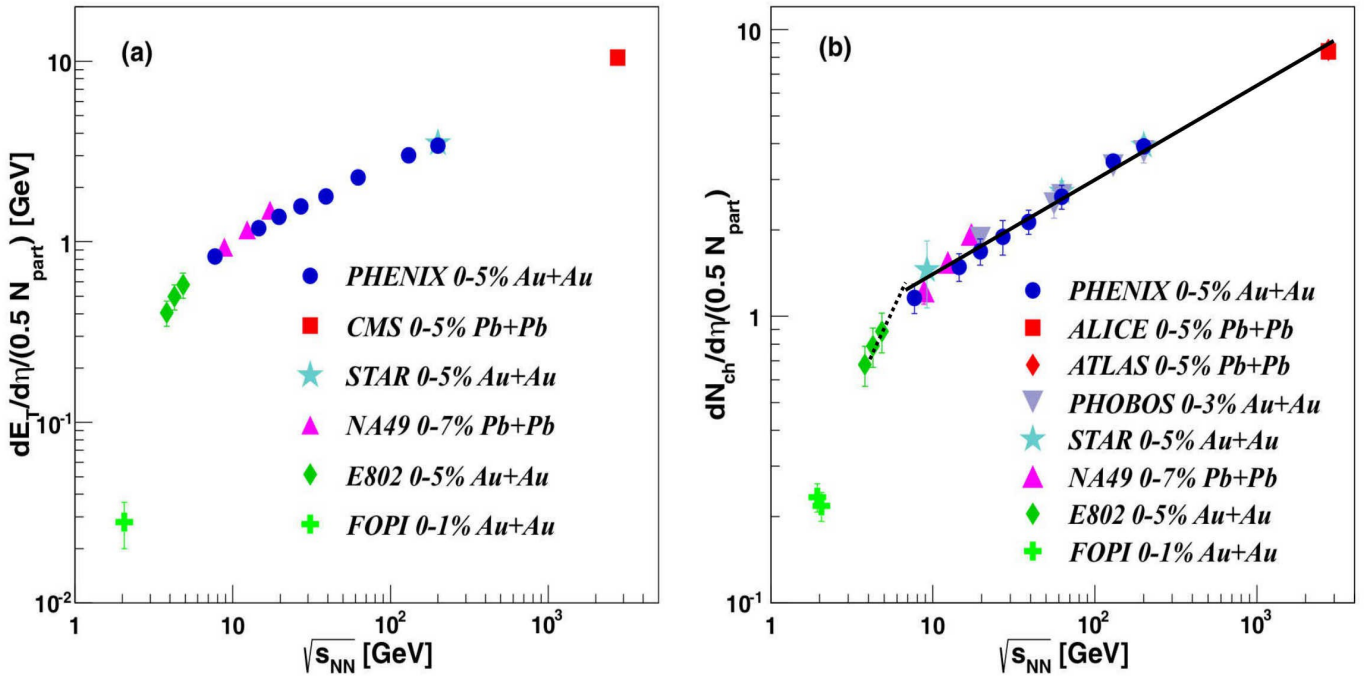

FIG. 4. The excitation function of $(dE_T/d\eta)/(0.5N_{\rm part})$ (a) and $(dN_{\rm ch}/d\eta)/(0.5N_{\rm part})$ (b) for central collisions at midrapidity as a function of $\sqrt{s_{NN}}$. The error bars represent the total statistical and systematic uncertainties. For $(dE_T/d\eta)/(0.5N_{\rm part})$ (a), data are shown from FOPI [28], E802 [29], NA49 [30,31], STAR [18], and CMS [31]. For $(dN_{\rm ch}/d\eta)/(0.5N_{\rm part})$ (b), data are shown from FOPI [28], E802 [29,32,33], NA49 [30], STAR [18,34], PHOBOS [17], ALICE [35], and ATLAS [36].

Charged particle multiplicity appears to follow power law $E_{cm}^{1/3}$ ($s^{1/6}$) at high energy (above 10 GeV) and linear ($s^{1/2}$) dependence below 10 GeV.

Transverse energy per particle changes very slowly. Total energy emitted via charged particle channels does not scale with beam energy !
Limit on entropy production ?

Linear dependence below 10 GeV: Statistical emission ?

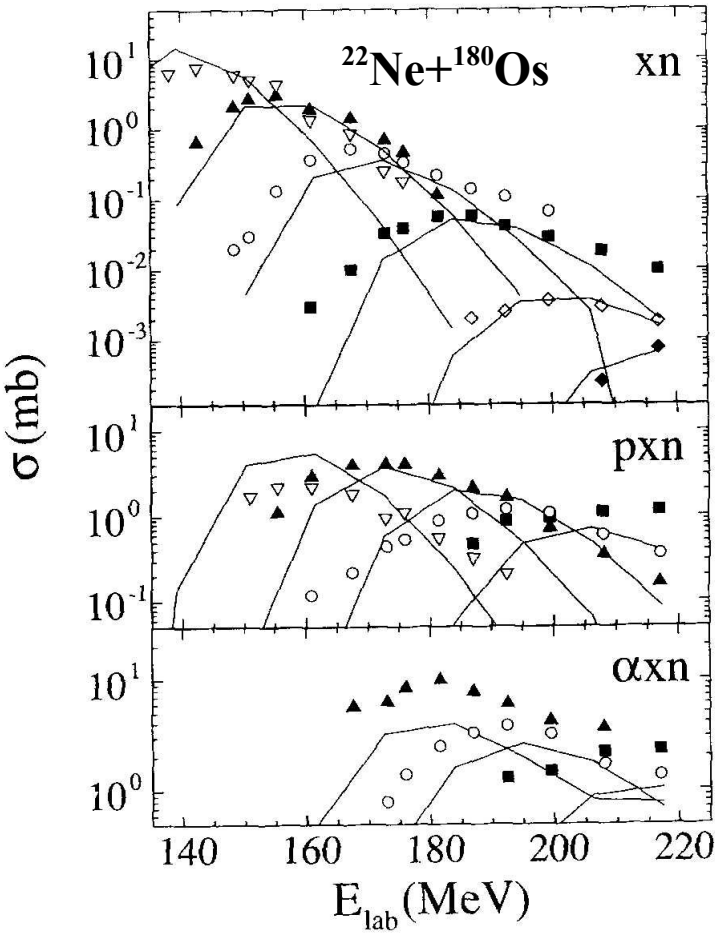

Similar situation observed in complete fusion at low energy !

Multiplicity of emitted neutrons grows linearly with c.m. excitation energy.

Statistical models of hadron emission :

Fermi (phase-space) – $E_{cm}^{3/4}$

Landau (covariant) – $E_{cm}^{2/3}$

Hagedorn (bootstrap) – linear !

Experimental multiplicity of pions in nucleon-nucleon collisions grows linearly with c.m. energy.

Combined with Glauber picture also multiplicity of pions in nucleus-nucleus collisions should grow linearly, as observed in experiment.

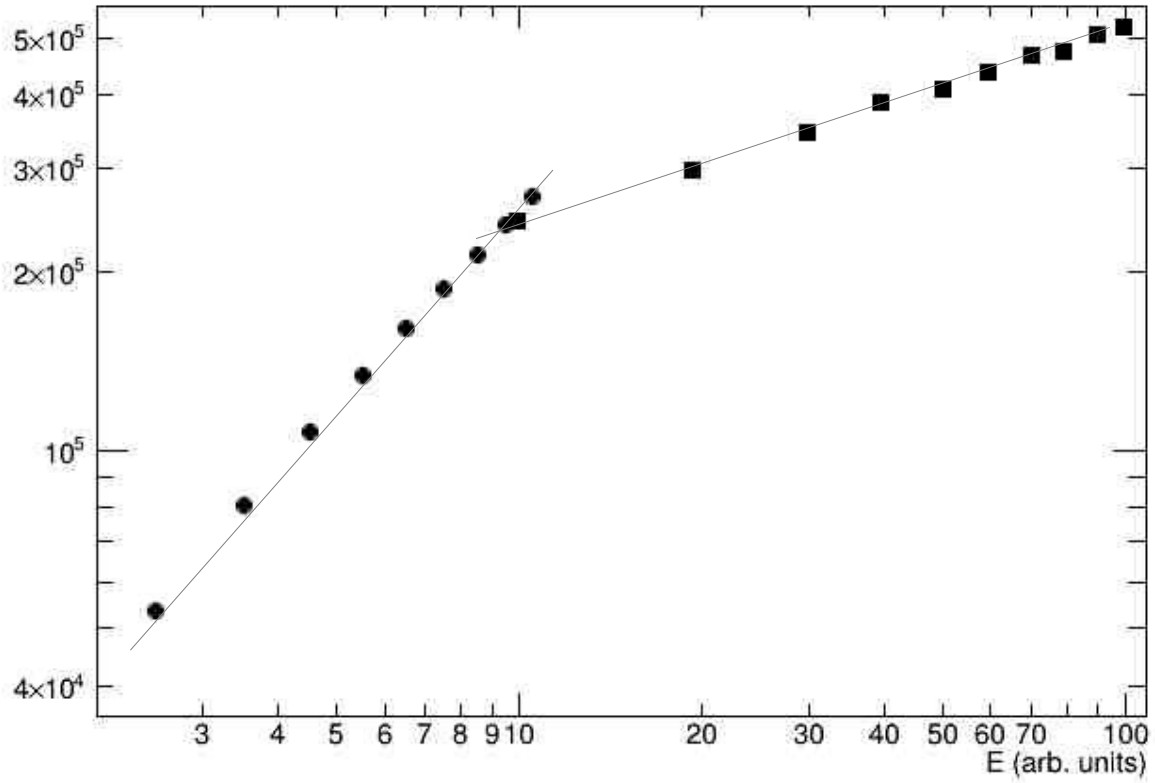

Schematic model simulation

1. Glauber picture, collision in center of mass frame.
2. Linear multiplicity in nucleon-nucleon collisions
3. Above some threshold energy, tube-like potential barrier applied, thus only 1D phase space along beam direction is filled and $E_{cm}^{1/3}$ dependence emerges.

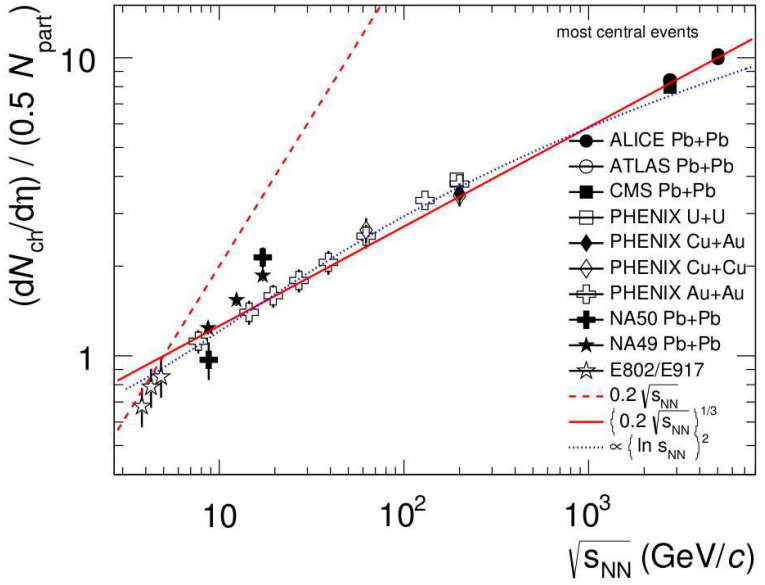

FIG. 1. Excitation function of pseudorapidity density of charged particles per participating nucleon pair in heavy-ion collisions [1, 3–10, 14]. Data points are for most central collisions. See text for more details.

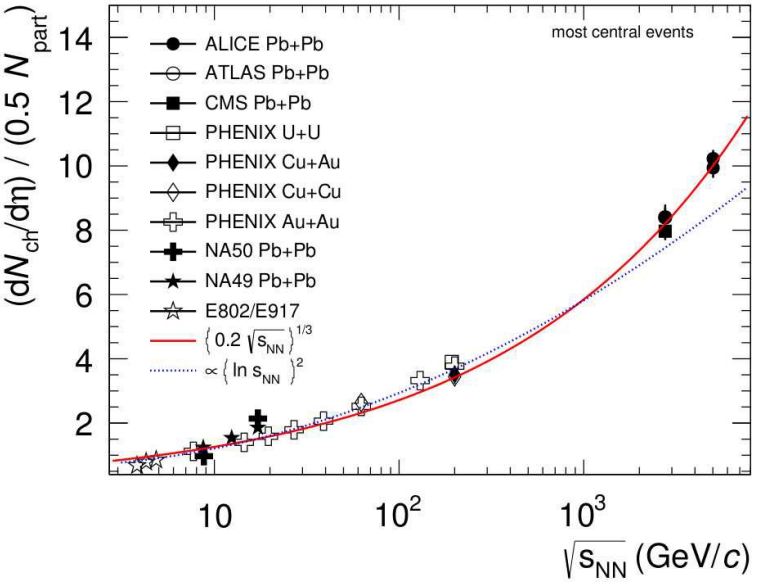

FIG. 2. Same as Fig. 1 but shown with linear multiplicity axis emphasizing the comparison of the parametrizations of the excitation functions at the LHC energies.

Data from LHC show that for central collisions $E_{cm}^{1/3}$ ($s^{1/6}$) fit is good (see above) while the empirical $(\ln s)^2$ fit previously proposed by PHOBOS collaboration fails.

$E_{cm}^{1/3}$ ($s^{1/6}$) fit reproduces also data from peripheral collisions (see right)!

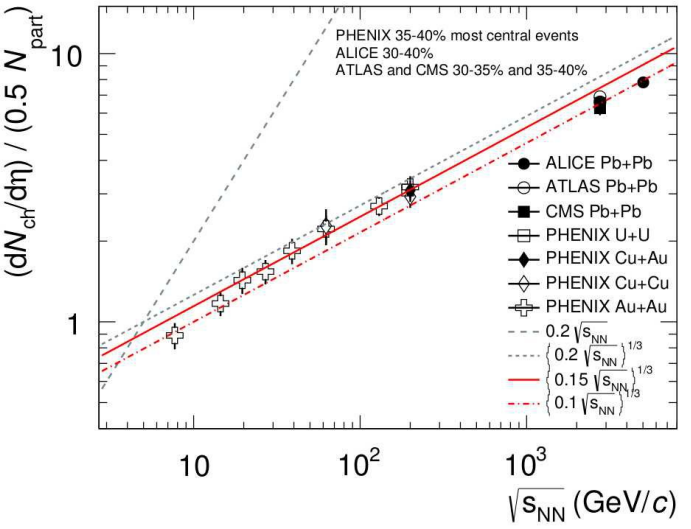

FIG. 3. Excitation function of pseudorapidity density of charged particles per participating nucleon pair in semi-central heavy-ion collisions [1, 3, 5, 6, 14]. See text for details.

Thus concerning multiplicity in nucleus-nucleus collisions at ultra-relativistic energies it appears that:

1. Topology of phase space changes from 3D to 1D.

2. Data above c.m. energy 10 GeV and $(dN_{ch}/d\eta)/(0.5N_{part}) = 1$ represent deconfined matter.

3. Location of critical point can be estimated around $s^{1/2} = 10$ GeV.

4. Limitations on entropy production are observed.

Summary and conclusions

Nucleus-nucleus collisions allow to investigate nuclear equation of state in wide range of incident energies from Coulomb barrier to LHC energies

Measured cross sections of super-heavy nuclei allow to extract limitations of incompressibility and density dependence of symmetry energy

Limitations for incompressibility and density dependence of symmetry energy extracted within a range of density up to five times saturation density

Trends of viscosity exhibit transition from liquid-like to gas-like behavior

Trends of charged particle multiplicity in ultra-relativistic nucleus/nucleus collisions appear to manifest change in topology of phase space (3D to 1D)

Entropy production appears to be limited

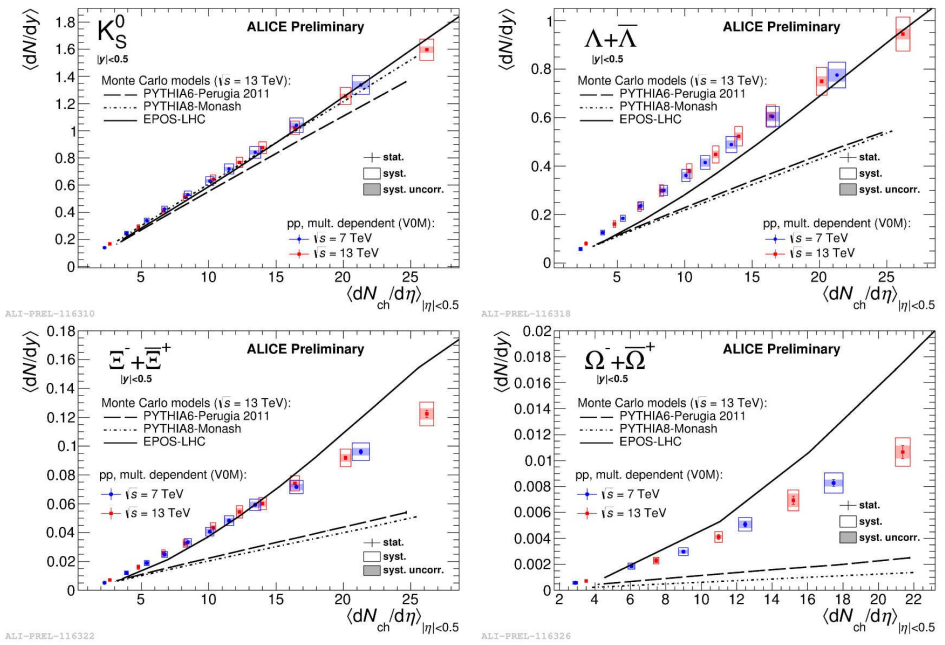

Fig. 2. p_T-integrated K^0_S, $\Lambda + \bar{\Lambda}$, $\Xi^- + \bar{\Xi}^+$ and $\Omega^- + \bar{\Omega}^+$ yields as a function of charged particle multiplicity at $|\eta| < 0.5$ measured in pp collisions at $\sqrt{s} = 7$ (red) and 13 (blue) TeV with comparison to EPOS-LHC [14] and PYTHIA6/PYTHIA8 [6] predictions.

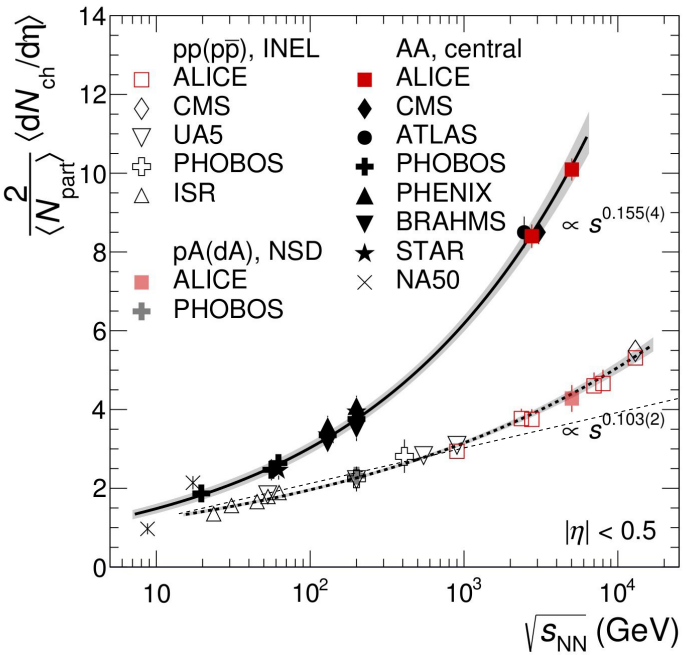

pp collisions at LHC

Strangeness scales with multiplicity, signal of deconfinement (ALICE)

Total multiplicity shows deviation from logarithm of energy, also signal of QGP onset ?

Table 1: Overview of principal production mechanisms of charged hadrons depending on collision type and beam energy

Collision type	Beam energy ($\sqrt{s}$)	Multiplicity trend	Reaction mechanism
e^+e^-	10 - 100 GeV	$\sqrt{E_{beam}}$ ($s^{1/4}$)	Fragmentation of isolated jets (Tube model of Feynman)
$p+p,\ p+A$	10 GeV - 1 TeV	$ln\ E_{beam}$ ($ln\ s^{1/2}$)	Fragmentation of jets in spectator matter (Uncorrelated jet model)
$p+p,\ p+A$	$>$ 1 TeV	faster than $ln\ E_{beam}$	Onset of deconfined matter ?
$A+A$	$<$ 10 GeV	linear ($s^{1/2}$)	Hadronic cascade (3D phase space)
$A+A$	$>$ 10 GeV	$E^{1/3}_{beam}$ ($s^{1/6}$)	Deconfined matter (1D phase space)